This is a postprint version of the following published document:

Sarasini, F., Tirillò, J., Lampani, L., Barbero, E., Sanchez-Saez, S., Valente, T., Gaudenzi, P. & Scarponi, C. (2018). Impact behavior of sandwich structures made of flax/epoxy face sheets and agglomerated cork. *Journal of Natural Fibers, 17*(2), 168-188

Impact behavior of sandwich structures made of flax/epoxy face sheets and agglomerated cork

F. Sarasini[a], J. Tirillò[a], L. Lampani[b], E. Barbero[c], S. Sanchez-Saez [c], T. Valente[a], P. Gaudenzi[b], and C. Scarponi[b]

[a]Department of Chemical Engineering Materials Environment, Sapienza-Università di Roma and UDR INSTM, Roma, Italy; [b]Department of Mechanical and Aerospace Engineering, Sapienza-Università di Roma, Roma, Italy; [c]Department of Continuum Mechanics and Structural Analysis, University Carlos III of Madrid, Madrid, Spain

ABSTRACT

The unremitting quest of natural and renewable materials able to replace their synthetic counterparts in high-performance applications has involved also sandwich structures. In this regard, the aim of this work is to characterize the impact response, in both high- and low-velocity conditions, of green sandwich structures made of agglomerated cork as core and flax/epoxy laminates as face sheets. Both bare cork, flax skins, and complete sandwich structures were subjected to impacts at three different energy levels representing the 25%, 50%, and 75% of the respective perforation thresholds. A gas gun was instead used to assess the high-velocity impact behavior of these green sandwich structures and evaluate their ballistic limit. This study shows that the buckling of cell walls of agglomerated cork enables to tailor the damage extension through-the-thickness in low-velocity impacts compared to traditional synthetic foams coupled with a considerable amount of energy absorption.

Introduction

The last two decades have witnessed a resurgent interest in materials from renewable resources due to the need to mitigate the environmental impact of energy-intensive production processes of synthetic fibers and polymers and to increase the recyclability and end-of-life disposal options of lightweight structures (Akampumuza et al. 2016; Faruk et al. 2012; Fowler, Mark Hughes, and Elias 2006; Gurunathan, Mohanty, and Nayak 2015; Ku et al. 2011; Mittal, Saini, and Sinha 2016). A typical representative of lightweight structures is the composite sandwich structure, which couples high flexural stiffness, low weight, thermal and acoustic insulation and flexibility in selection from a broad range of materials. Nowadays these structures are widely diffused as semi- or structural

components in many industrial fields. A general concern associated with traditional sandwich structures is their poor response to impact loading as the resulting damage scenario, compared to composite laminates, is complicated by multiple damages potentially occurring in the face sheets (delamination and fiber breakage), at the face sheet/core interface region (debonding) and in the core (crushing and shear failure) (Abrate 1997; Wang, Waas, and Wang 2013; Zenkert et al. 2005; Zhou et al. 2012). Standard core materials are represented by honeycombs, foams, and balsa wood, but recent developments have resulted into new alternatives, such as natural materials with cellular morphology with particular emphasis on cork (Alcântara, Teixeira-Dias, and Paulino 2013; Castro et al. 2010; Paulino and Teixeira-Dias 2011). In this regard, agglomerated cork, which is a mixture of natural cork and an organic binder (typically polyurethane), can be considered as an alternative to synthetic foams currently used in structural applications with a significant energy absorption ability. In addition, cork shows reduced permeability to liquids and gases and thermal insulation properties with a distinctive mechanical behavior resulting in nonlinear elasticity, exceptional compressibility without fracture, and unusual dimensional recovery capability, which enables outstanding energy-absorbing performance (Sargianis, Kim, and Suhr 2012; Silva et al. 2005; Pereira 2007; Fernandes, Pascoal, and Alves de Sousa 2014; Triantou et al. 2017; Zhuang et al. 2017; Barbosa et al. 2017). Several studies on cork and related sandwich structures are available in literature but with a strong focus on quasi-static properties, such as compression, tensile, and shear (Gameiro, Cirne, and Gary 2007; Mancuso, Pitarresi, and Tumino 2015; Alcântara, Teixeira-Dias, and Paulino 2013; Moreira, De Melo, and Dias Rodrigues 2010; Reis et al. 2007; Reis and Silva 2009; Oliveira, Rosa, and Pereira 2014). A less investigated issue is the response of agglomerated cork and its sandwich structures to impact loading. Sanchez-Saez, García-Castillo, et al. (2015) investigated the effect of thickness on the dynamic crushing behavior of agglomerated cork using an instrumented drop weight tower. The authors found that maximum contact force, maximum displacement, and maximum strain exhibited a large dispersion likely ascribed to the natural origin of agglomerated cork. An increase in the specimen thickness caused a reduction of the contact force for the same impact energy and the energy absorbed by the specimens represented a high percentage of the impact energy. In addition, a linear relationship between the absorbed energy and the impact energy/thickness ratio for each specimen thickness (15–70 mm) was pointed out, while no significant dependence of the energy-absorption capability of the agglomerated cork on the thickness was found. Due to the viscoelastic behavior of agglomerated cork, Sanchez-Saez et al. (2015) analyzed the behavior of agglomerated cork of different thickness (35, 50, and 70 mm) when subjected to three consecutive impacts of energy equal to 17.5 and 35 J. The results highlighted that the energy absorption was significant after every impact and that the absorbed energy did not depend on the number of impacts as only a decrease in the range 3–6% was detected between the first and third consecutive impact. Sousa-Martins et al. (2013) addressed the response of sandwich structures incorporating agglomerated cork as core between two aluminum alloy face sheets to blast waves originated from the detonation of 30 g of explosive (C4). The authors reported a value of about 11% for the relative thickness reduction, thus suggesting the possibility of energy dissipation by the core through crushing of the cellular structure of cork. Sanchez-Saez, Barbero, and Cirne (2011) discussed the behavior of agglomerated cork subjected to ballistic impacts using a gas gun. Three different configurations were tested, namely an agglomerated cork 37 mm thick, two thin aluminum alloy (6063-T5) plates (1.8 mm) and spaced 37 mm, and a pair of thin aluminum alloy plates separated by agglomerate cork. The ballistic limit of agglomerated cork (160 m/s) was lower than that of the aluminum alloy plates (323 m/s), but when the agglomerated cork was used as core between the two aluminum alloy plates, the ballistic limit increased by a 7.7% (348 m/s) along with absorbed energy at impact velocities that caused perforation. Petit et al. (2007) investigated the low-velocity impact behavior of composite laminates (carbon/epoxy) with and without cork thermal shield. The authors found that the thermal protection acted as a mechanical protection with damage that appeared at higher impact energies for shielded laminates. However, above a certain impact energy threshold, they reported the possibility to have more important delaminated areas for shielded panels than for unshielded ones. From a

literature survey, the use of carbon/epoxy laminates or aluminum alloys as face sheets in sandwich structures based on agglomerated cork emerged, thus limiting the full exploitation of the environmentally friendly character of cork. Hachemane et al. (2013) reported results of an experimental characterization of a jute/epoxy–cork sandwich material to impact and indentation manufactured by one-shot infusion. Three cork densities were studied, namely 160, 270, and 310 kg/m^3, and this parameter was found to affect the impact response. With increasing density, the maximum force recorded decreased of about 60%, which was ascribed to the resin infiltration in the pores of the agglomerated cork that led to an increased material local stiffness. In addition, the increment of cork density caused also a reduction of 3.72% in the energy dissipation capacity for a 7 J impact. Recently, Walsh et al. (2017) characterized a sandwich structure based on carbon fiber face sheets and expanded cork and compared the results with those of structures based on Rohacell® 110 IG. The authors found that, when compared to the synthetic foam, expanded cork showed a decrease in bending stiffness, but a large improvement in acoustic, damping, and impact damage resistance characteristics. In particular, for a 10 J impact, the expanded cork showed a significantly smaller dent depth, less damage to the core and top face sheet, and no damage to the bottom face sheet compared to the synthetic counterpart. Other authors (de Moura et al. 2017, 2015; Silva, de Moura, and Magalhães 2017) recently proposed the use of cork layers at selected interfaces to increase the interlaminar fracture resistance of a carbon fiber-reinforced composite. In particular Silva, de Moura, and Magalhães (2017) addressed the low-velocity impact behavior of a monolithic cross-ply carbon-epoxy laminate and a hybrid one made of carbon-epoxy and a cork layer placed in the most critical interface. Contrarily to monolithic laminate where a longitudinal crack and large delamination developed, the hybrid solution revealed a larger longitudinal crack without any evidence of extensive delamination at the cork layer. This was ascribed to the dissipation of impact energy in a large fracture process zone that can be developed inside the cork layer. No studies addressing at the same time the low- and high-velocity impact behavior of green sandwich structures can be found in the available literature. To bridge this gap, the aim of the present work is to analyze the response to low- and high-velocity impacts of green sandwich panels consisting of flax/epoxy face sheets and agglomerated cork. For qualitative comparison purposes, a traditional Rohacell 110WF rigid foam has been also used with the same flax/epoxy face sheets. Foam core has been chosen only because it represents a standard in industrial applications and can act as a reference material with a very well-known behavior. This greener sandwich construction has been scarcely investigated, with the exception of the work by Mancuso, Pitarresi, and Tumino (2015), where an in-depth quasi-static characterization in bending was addressed without considering the response to impulsive loadings.

Materials and methods

Materials and fabrication of sandwich structures

Two different sandwich structures were investigated and compared in this experimental work, both characterized by the same flax/epoxy face sheets and different core materials. For the skins, a unidirectional prepreg material system (FLAXPREG UD 180) based on epoxy matrix with a fiber areal weight of 180 g/m^2 supplied by Lineo was used. Two face sheets encapsulated a core of agglomerated cork (ECOPAN) supplied by Etruria Cork Srl with a nominal density of 145 kg/m^3 and a thickness of 30 mm. It is worth noting that this is a product used in the building industry as thermal and acoustic insulating material, therefore not specifically optimized for applications in composites. To benchmark the performance of this green sandwich structure, a similar sandwich with a closed-cell rigid foam based on polymethacrylimide (PMI), namely Rohacell® 110WF supplied by Evonik Industries AG, was manufactured. This foam core has been provided with a density of 110 kg/m^3 and a thickness of 30 mm. The face sheets were manufactured with a quasi-isotropic configuration [+60/0/−60]$_s$ and the panels were vacuum-bagged and fully cured under pressure in an

autoclave to the manufacturer's specifications up to a fiber volume fraction of ~0.50 ± 0.04. The flax fiber laminates with a thickness of 1.4 mm and the two different cores were cut to required dimensions (10 × 10 cm) and Redux 609 by Hexcel, an epoxy film adhesive containing a cotton scrim, was used to bond the face sheets to the core. Sandwich structures were vacuum-bagged and fully cured without additional pressure in an autoclave to the epoxy film manufacturer's specifications.

Quasi-static characterization techniques

Flax/epoxy face sheets were tested for tensile and flexural properties in accordance with ASTM D3039 and ASTM D790, respectively. Tensile tests were carried out with a cross-head speed of 2.5 mm/min, and the deformation was recorded by an extensometer with a gage length of 50 mm. Three-point bending tests were performed with a support span of 60 mm and a cross-head speed of 4 mm/min. At least three specimens were tested. Both core materials were characterized in static compression tests with at least five specimens (30 × 30 × 30 mm) at three test velocities, namely 5, 10, and 50 mm/min. All the quasi-static tests were carried out using a Zwick/Roell Z010 testing machine.

Dynamic characterization techniques

Core materials, face sheets, and the whole sandwich structures were subjected to low-velocity impact tests using an instrumented drop-weight impact testing machine (CEAST/Instron 9340). The hemispherical impactor had a diameter of 20 mm, and the dropped carriage had a total mass of 3 kg for flax/epoxy face sheets and 8 kg for the remaining samples. The specimens were pneumatically clamped between two steel plates, leaving a circular unsupported area with a diameter of 40 mm. At first low-velocity impact tests were performed up to perforation for cores, face sheets, and sandwich structures, and then tests were carried out at different percentages of the respective perforation energy, namely 25%, 50%, and 75%. As many parameters (density, cell size, cork grain size) can in principle affect the impact response of such sandwich structures, it is difficult to compare two materials with exactly the same characteristics especially if one takes into account the large variability in density of commercial agglomerated corks due to the natural origin of the material. The comparison reported in this work is deemed to provide useful insights into the deformation and failure mechanisms of these different sandwich structures. This also explains the need to impact the specimens at different percentages of their respective perforation energies without using the same absolute impact energy levels in an attempt to limit the influence of differences in materials properties. At least three specimens were impacted for each combination of material and energy level.

The high-velocity impact tests were performed using an A1G+ gas gun by Sabre Ballistic. Twelve specimens for each sandwich configuration were impacted by a spherical tempered steel projectile (mass = 1.725 g, diameter = 7.5 mm) over a range of impact energies until complete perforation of the target. A high-pressure gas (argon) provided the force to impulse the projectiles. Impact velocity was varied by changing the pressure in the gas gun.

The samples were mounted in a simply supported boundary condition along their edges by aluminum guides. In order to measure impact and residual velocity, the tests were monitored using a high-speed digital camera APX FASTCAM by Photron with a data acquisition system set to take 36,000 frames per second placed beside the sample holder. After determining the speeds of the projectile before and after impact using the high-speed camera, the experimental data have been fitted by least-square regression according to the classical Lambert–Jonas equation (Lambert and Jonas 1976; Sanchez-Saez, Barbero, and Cirne 2011) to obtain the ballistic limit velocity.

Microstructural investigation

The morphology and structure of core materials and flax/epoxy face sheets were examined by scanning electron microscopy (SEM) (Philips XL 40). The specimens were sputter coated with gold prior to investigation.

Results and discussion

Morphological characterization

The morphology and structure of agglomerated cork and Rohacell foams were first examined and compared. Figure 1 shows the morphology of both core materials. Being cellular materials in nature, both exhibited a similar microstructure but with some distinctive features. In fact, while Rohacell foam can be described by cell sizes ranging from 610 to 836 μm, the cork used in the present study showed relatively large grains (4–8 mm) and a significantly smaller cell size of approximately 28–43 μm. Moreover, cork displayed a smaller cell wall thickness of about 1.26 μm compared to 22.31 μm of 110 WF. These morphological features need to be taken into account as it has been shown that agglomerated corks can exhibit dissimilar mechanical properties depending not only on density, but also on the agglomerated grain size, the amount of binder, and even on the processing method (Jardin et al. 2015).
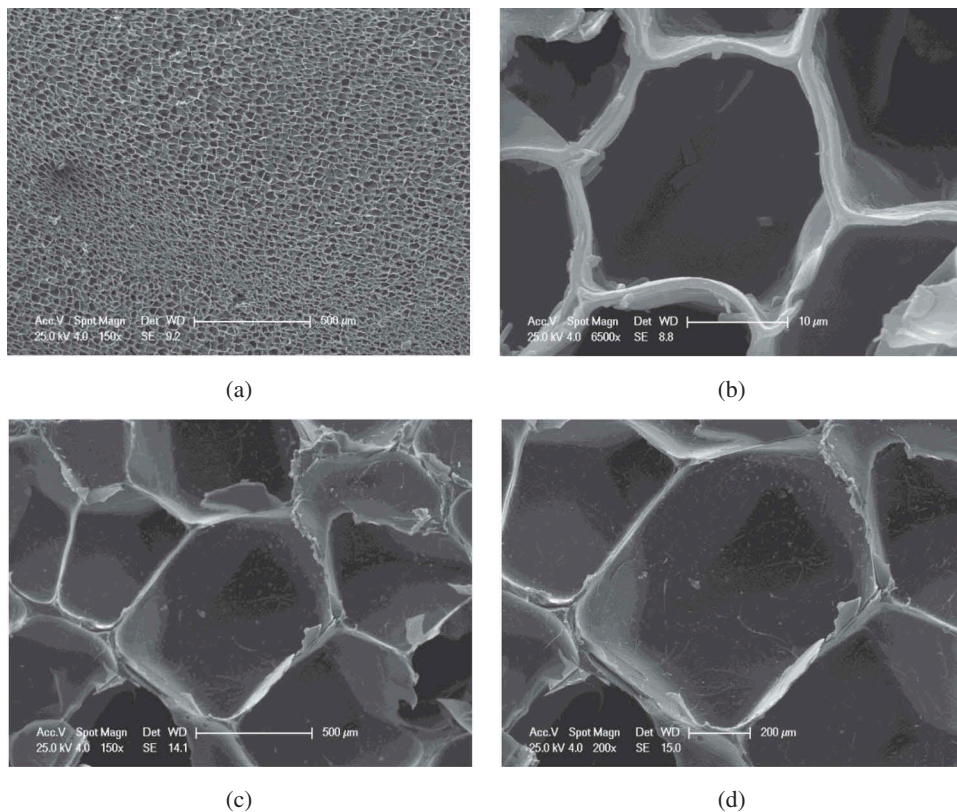

(a)

(b)

(c)

(d)

Figure 1. SEM micrographs of agglomerated cork (a, b) and Rohacell (c, d) at different magnifications.

Quasi-static mechanical properties of single constituents

Typical stress–strain curves obtained from compression tests on cork and synthetic foam are reported in Figure 2. As extensively reported in literature (Fernandes, Pascoal, and Alves de Sousa 2014; Gibson and Ashby 1999), stress–strain curves displayed the common three compression stages, indicated by numbers in Figure 2, which are (1) linear elasticity at low stresses due to cell wall bending, (2) a long collapse plateau due to elastic buckling of cell walls in cork and brittle crushing in synthetic foam, and (3) densification stage where the collapse of cells and compaction of the successive cell walls occur. From the curves in Figure 2, the compressive modulus (evaluated from the average slope of the stress–strain curve in the elastic stage) and the collapse stress (evaluated as the intersection of the lines fitting the plateau and the elastic stages) were obtained and reported in Figure 3. As a general comment, both materials exhibited a reduced dispersion in properties, which is quite remarkable for agglomerated cork as its behavior is anisotropic with higher strength in the radial direction compared to the axial and tangential directions (Pereira 2007). Despite the relatively large grain sizes, the different and random grain orientations inside the agglomerated cork are envisaged to be responsible for this reduced variability and quasi-isotropic behavior. Synthetic foam clearly outperformed the agglomerated cork in terms of strength and stiffness at every test speed. It is worth noting that both core materials exhibited a strain rate sensitivity described by an increase of
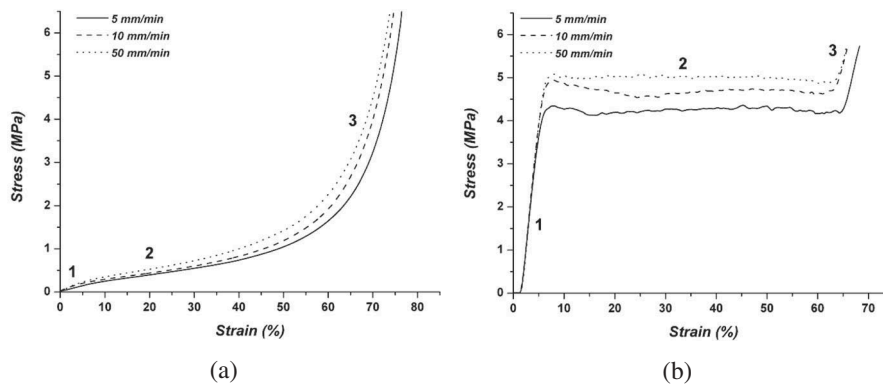

Figure 2. Representative compression stress–strain curves for (a) cork and (b) synthetic foam as a function of test velocity.
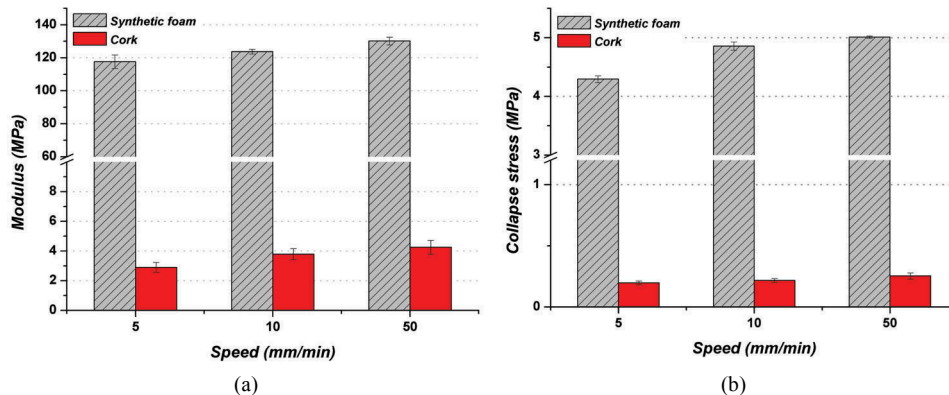

Figure 3. Compressive modulus and collapse stress for cork and synthetic foam as a function of test speed.

collapse stress and stiffness with increasing test speed, albeit not so marked at least in the velocity range investigated in the present study.

The tensile and flexural properties of flax/epoxy face sheets are summarized in Table 1. These results compare quite favorably with previous research, where tensile strengths of flax/epoxy composites have been reported in the range 60–120 MPa (George, Verpoest, and Ivens 1999; Goutianos et al. 2006; Meredith et al. 2013; Phillips et al. 2013; Sarasini et al. 2016). Fracture surfaces of composites (Figure 4) showed that there is still room for improvement with regard to the fiber/matrix interface even if no clear gaps between fiber and matrix and fiber fibrillation can be noted.

Low-velocity impact behavior

Before testing the whole sandwich structures, bare core materials and flax/epoxy face sheets have been subjected to low-velocity impact tests. Transient data were collected for each sample, including time, load, energy, velocity, and displacement. Figure 5 illustrates the load versus displacement plots of representative flax/epoxy face sheets as a function of increasing impact energy up to perforation. It is possible to note that even at the lowest impact energy the transient response of the samples showed load drops indicating a certain amount of damage, with increasing tendency up to 75% of

Table 1. Summary of mechanical properties for flax/epoxy face sheets.

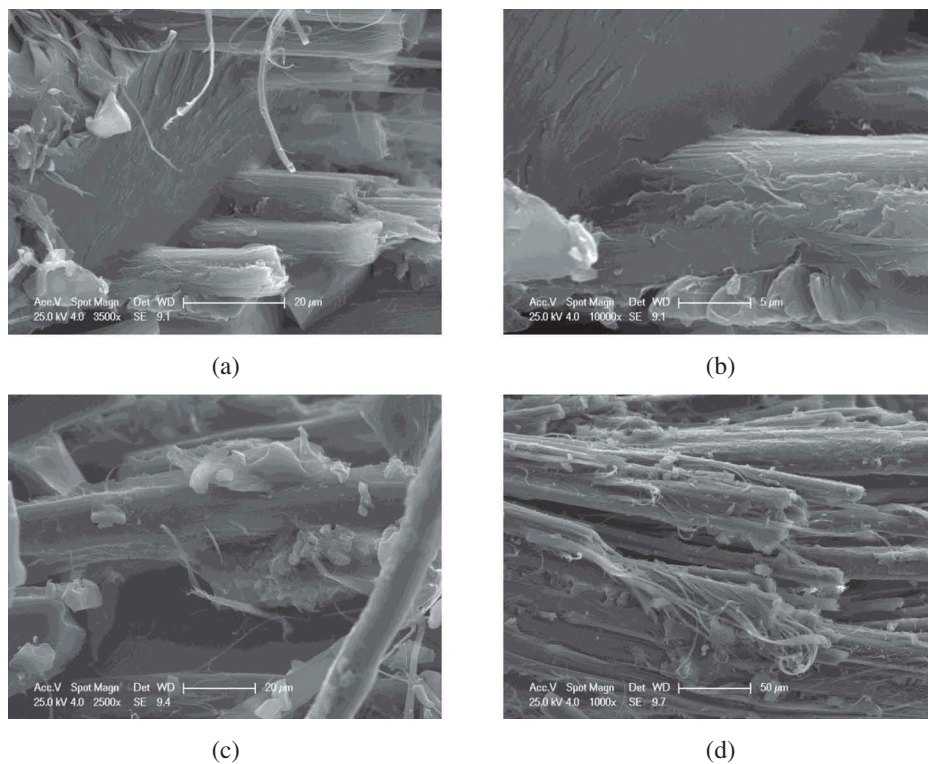|	Tensile strength (MPa)	Tensile modulus (GPa)	Flexural strength (MPa)	Flexural modulus (GPa)
Flax/epoxy face sheet	117.86 ± 3.49	12.71 ± 0.34	91.95 ± 2.79	7.20 ± 0.26

(a)

(b)

(c)

(d)

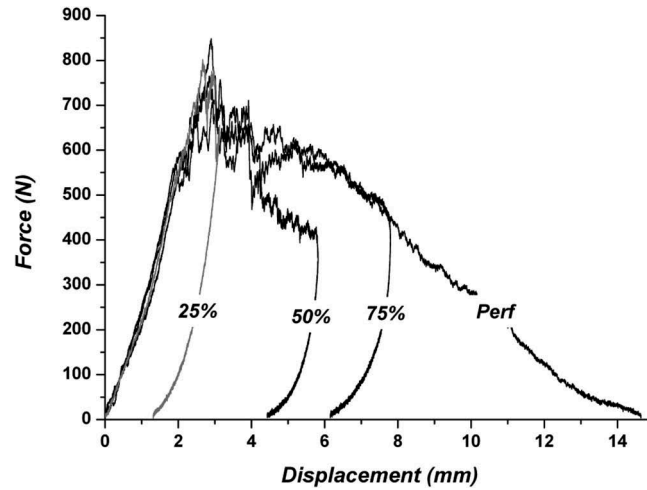**Figure 4.** SEM micrographs of fracture surfaces of flax/epoxy composites.

Figure 5. Characteristic force versus displacement curves for bare flax/epoxy face sheets.

the perforation energy (E_p), which was found to be quite low (Table 2). The peak load increased with the increase in the impact energy up to 50% of the perforation energy and dropped for an impact energy equal to 75% of E_p where the laminates experienced severe damage, as confirmed by a damage degree (defined as the ratio between absorbed energy and impact energy) close to unity, when penetration occurs. The damage evolution on the front and rear surfaces of flax/epoxy laminates is shown in Figure 6. It is evident that already at 25% E_p marked delamination on the back surface is present with an oblong shape with its major axis coincident with the fiber direction of the layer below the interface. These delaminations are always associated to matrix cracks that represent the first damage appearing after an impact event, which are much more evident at higher impact energies on both front and rear surfaces (Figure 6). In thin and flexible laminates, it is reasonable to assume that bending stresses cause tensile failure of the bottom ply in the transverse direction because membrane effects are predominant. It is this preliminary failure that induces

Table 2. Impact parameters for bare face sheets, core materials, and complete sandwich structures.

| Sample	Perforation energy (E_p) (J)	Peak force (N)	Maximum displacement (mm)	Absorbed energy (J)	Damage degree
Bare face sheet_Perf	5.20 ± 0.38	795.25 ± 89.44	–	–	1
Bare face sheet_25% E_p	–	893.57 ± 90.54	3.02 ± 0.14	0.77 ± 0.11	0.61 ± 0.09
Bare face sheet_50% E_p	–	940.73 ± 92.52	5.26 ± 0.78	2.36 ± 0.18	0.90 ± 0.06
Bare face sheet_75% E_p	–	753.09 ± 17.20	8.75 ± 1.36	3.88 ± 0.19	0.97 ± 0.03
Bare cork_Perf	9.69 ± 0.71	703.56 ± 3.74	–	–	1
Bare cork_25% E_p	–	515.51 ± 8.99	10.22 ± 1.33	2.41 ± 0.55	0.79 ± 0.08
Bare cork_50% E_p	–	577.44 ± 30.52	15.78 ± 2.97	5.50 ± 0.62	0.96 ± 0.04
Bare cork_75% E_p	–	747.71 ± 53.28	17.59 ± 4.10	7.06 ± 0.21	0.99 ± 0.02
Bare synthetic foam_Perf	37.41 ± 0.66	1982.53 ± 58.17	–	–	1
Bare synthetic foam_25% E_p	–	1596.03 ± 120.59	10.31 ± 0.54	–	1
Bare synthetic foam_50% E_p	–	1877.49 ± 136.11	15.57 ± 2.44	–	1
Bare synthetic foam_75% E_p	–	1880.20 ± 125.18	21.84 ± 3.51	–	1
Sandwich-cork_Perf	42.51 ± 0.95	2178.15 ± 127.51	–	–	1
Sandwich_cork 25% E_p	–	1633.47 ± 114.38	8.36 ± 0.40	9.21 ± 0.21	0.91 ± 0.02
Sandwich_cork 50% E_p	–	1764.12 ± 66.74	15.84 ± 0.82	–	1
Sandwich_cork 75% E_p	–	1784.78 ± 10.26	24.72 ± 1.11	–	1
Sandwich-foam_Perf	79.71 ± 2.24	3001.46 ± 160.03	–	–	1
Sandwich-foam_25% E_p	–	2401.69 ± 116.10	11.03 ± 0.43	–	1
Sandwich-foam_50% E_p	–	2430.89 ± 77.40	22.87 ± 1.53	–	1
Sandwich-foam_75% E_p	–	2730.28 ± 147.61	29.99 ± 1.46	–	1
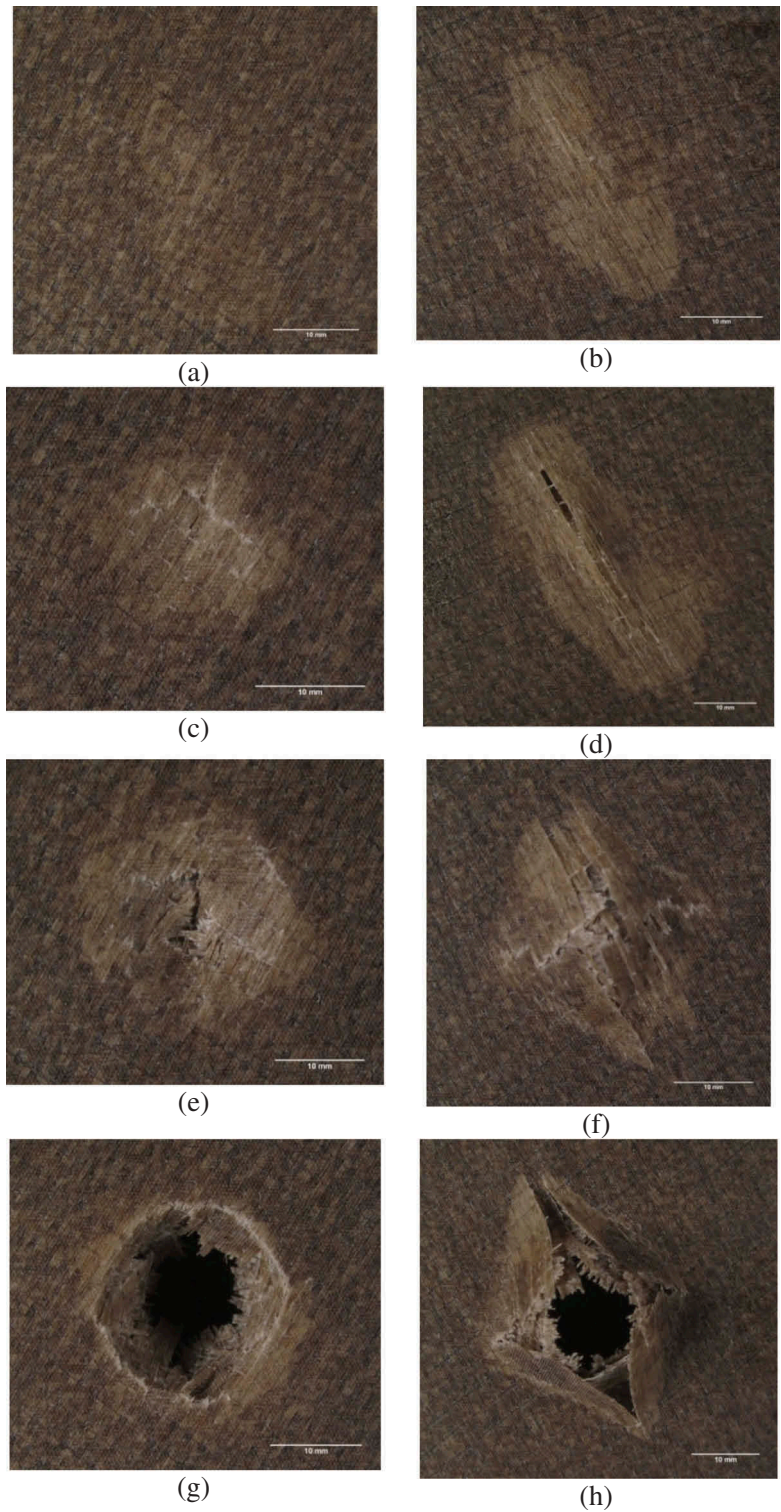
Figure 6. Close-up views of the damage progression in the front (left column) and back surfaces (right column) of flax/epoxy face sheets impacted at 25% (a, b), 50% (c, d), 75% (e, f), and up to perforation (g, h).

debonding of the first interface followed by a sequence of matrix cracks and delaminations (Ghelli and Minak 2011; Tita, de Carvalho, and Vandepitte 2008).

The behavior of bare cork and synthetic foam when subjected to low-velocity impact tests is compared in Figures 7 and 8 in terms of force–displacement curves while the impact parameters are summarized in Table 2. The two core materials exhibited different response to impact loading as can be inferred from the observation of transient data (Figures 7 and 8) and resulting damage modes (Figures 9 and 10). The agglomerated cork showed a clear rebounding phase at 25% of the perforation energy while at 50% some rebounding was still detected although the damage degree was about 0.96, thus suggesting imminent penetration. No rebounding was instead observed in synthetic foam specimens (Figure 8), which were characterized by penetration even at very low-impact energies. In both cases, peak load was found to increase with increasing impact energy. Synthetic foam specimens outperformed cork ones in terms of peak force, which is related to the plate stiffness (Richardson and Wisheart 1996), and perforation energy (E_p). Both properties are clearly influenced by the better mechanical properties of synthetic foam as already found during the
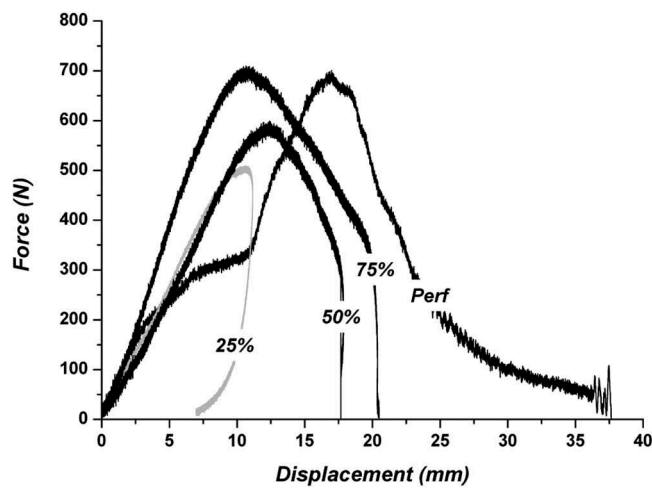

Figure 7. Typical force versus displacement curves of bare agglomerated cork impacted at different energy levels.
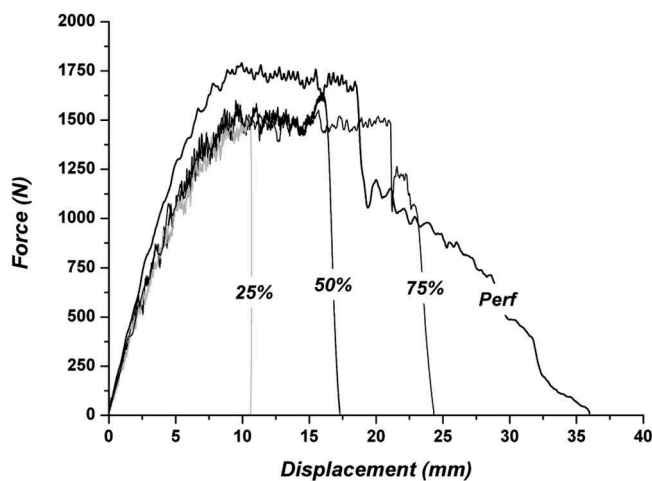

Figure 8. Typical force versus displacement curves of bare synthetic foam impacted at different energy levels.

quasi-static compression tests. The existence of a rebounding phase for cork specimens suggests less damage occurrence in the material. For both core materials, no damage in the back face was detected at all impact energies (25–75%), being all concentrated on the impacted surface. In the case of cork, samples impacted at 25% E_p did not show any sign of damage in both surfaces, while at 50% E_p a slight indentation, which increased in depth at 75% E_p, was noted (Figure 9). Foam specimens exhibited a different behavior, with a deep indentation in the front surface even at an impact energy of 25% E_p (Figure 10). As the bare cork samples were more compliant, they deflected more than the foam core samples. The energy absorbed through the creation of damage was also lower and mainly ascribed to elastic response and creation of local dent. In order to better understand the damage mechanisms induced by impact, samples were sectioned through the impact point and images of cross-sectional view of the damage area are reported in Figure 11. By comparing the cross sections of impacted specimens, the different energy absorption mechanisms can be highlighted. Cork speci- mens exhibited a slight indentation on the impacted surface coupled with cell wall collapse due to buckling while a deep indentation and an extended crushed zone were detected for synthetic foam, where no core shear and cracking up to impact energies ≤ 75% E_p occurred. To confirm these assumptions, samples impacted at 75% E_p were sectioned and observed under SEM (Figure 12). Cork cell walls experienced buckling, and due to the collapse of individual cork cells and densification of the cork agglomerate, the energy absorption at high strains can be quite considerable with no signs of cell walls breakage, thus suggesting an almost complete recovery of their original shape and size (Figure 12(a)). In foam samples (Figure 12(b)), due to the brittle nature of cells, they tended to break rather than collapse with no possibility of recovery.
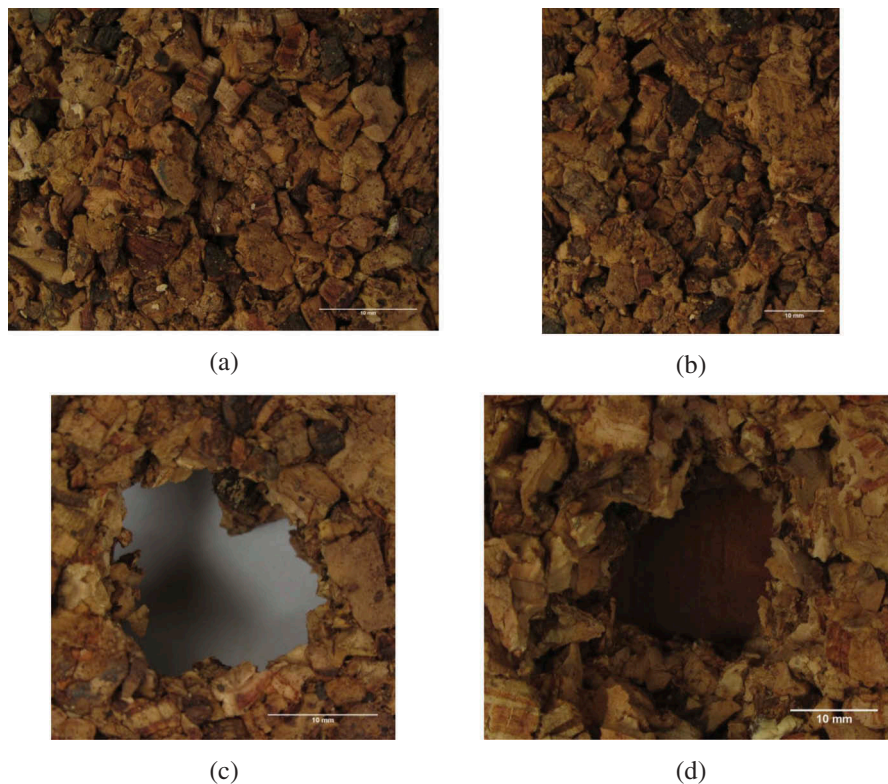

Figure 9. Close-up views of the damage progression in the front surfaces of bare cork impacted at (a) 50% E_p, (b) 75% E_p, and at perforation (c, d).
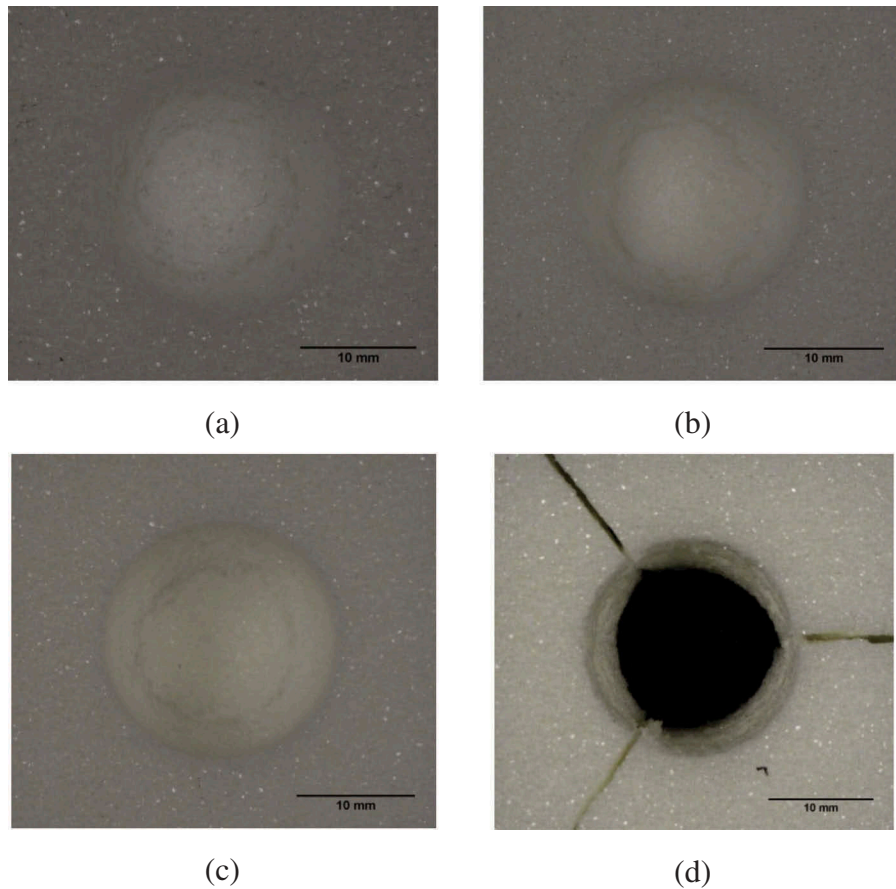
Figure 10. Close-up views of the damage progression in the front surfaces of bare synthetic foam impacted at (a) 25% E_p, (b) 50% E_p, (c) 75% E_p, and (d) at perforation.

These different damage modes are also responsible for the different responses found for the whole sandwich structures based on the two different cores, as shown in Figure 13. Also for complete sandwich structures, the different core material played a significant role, with cork that allowed a rebounding stage at least up to 25% of the perforation energy that was not observed for synthetic foam-based sandwich. Face sheets were perforated through fracture of the flax fibers (Figure 14), allowing the penetration of the impactor into specimens but force–displacement curves related to perforation were distinctly different. A curve with two peaks for cork-based sandwich structures was recorded (Figure 13(a)), implying the contact of the impactor with top and bottom face sheets, respectively, a feature that was not recorded for sandwich structures with synthetic foam (Figure 13(b)). It is also worth noting that the second peak value for cork-based sandwich samples is higher than the first peak value. The deformation characteristic of the cork core under compressive loading is likely to be the main cause of this behavior, which is in the form of collapsing of cells instead of breaking of cells (foam cracking). At higher strains, the cork cells have better energy absorption due to the collapse of individual cells and densification of the cork agglomerate structure that can resist further penetration of the impactor. As regards the synthetic foam (Figure 15(a)), no core shear and cracking for impact energies up to 75% of perforation energy were found and no bottom face sheet damage for impact energies up to 75% E_p for both sandwiches occurred (Figure 15). It is also to be noted the lower damage degree for neat cork and resulting sandwich compared to the synthetic foam, coupled with a lower through-the-thickness damage extension.
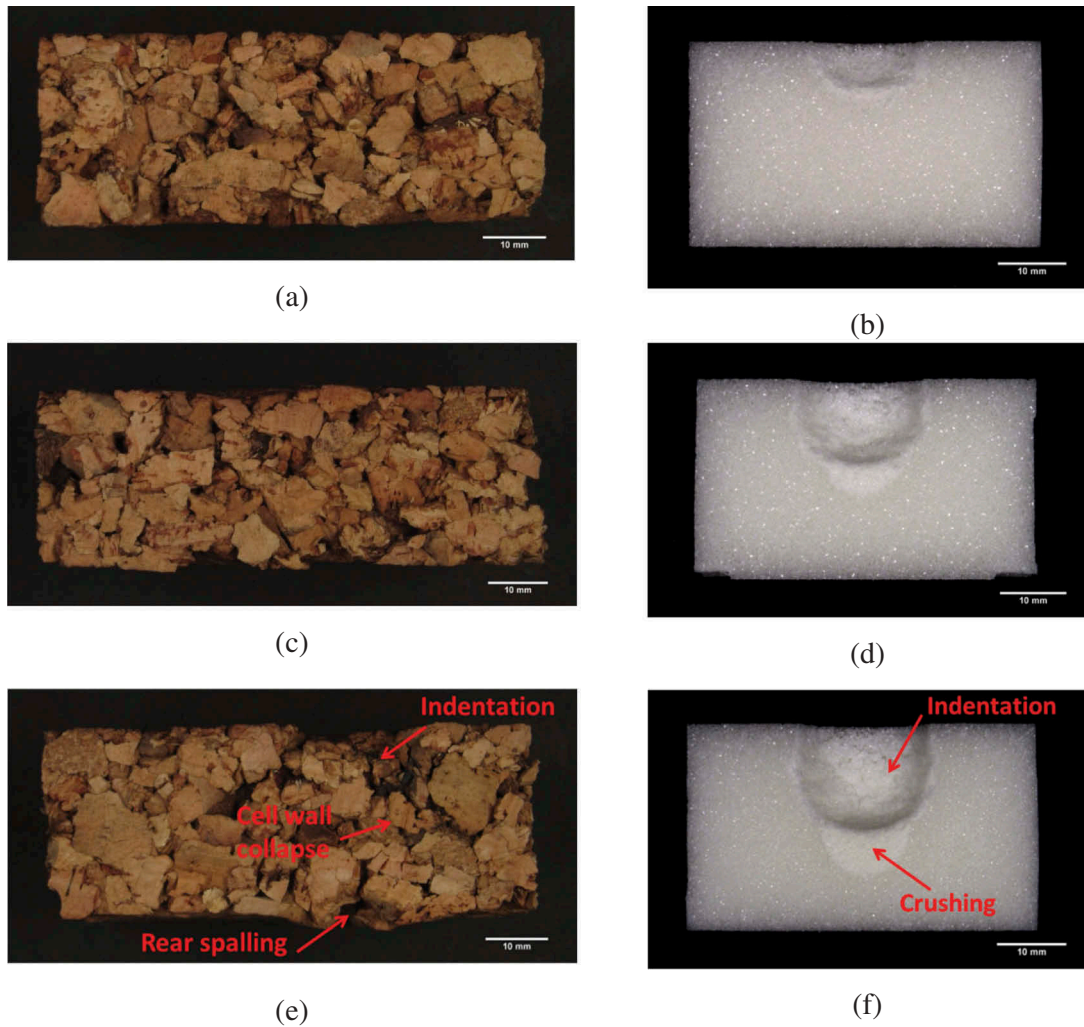
Figure 11. Cross-sectional views of bare (a, c, e) cork and (b, d, f) synthetic foam specimens impacted from 25% to 75% E_p (from top to bottom).

It is very difficult to provide a sound comparison of the data obtained in the present study with those available in literature on additional cellular materials, especially for low-velocity impact behavior. It is worth mentioning that many different parameters influence the response of sandwich structures to low-velocity impact. In fact, there are both material-based (including the type of constituents, foam density, the stacking sequence) and geometry-based parameters (for instance, size effect of test specimens and impactor's size/mass, geometry, velocity, clamping conditions, test area under impact) (Wang, Waas, and Wang 2013).

High-velocity impact behavior

In an attempt to confirm the energy absorption capability of agglomerated cork, its influence on the behavior of flax/epoxy face sheets subjected to high-velocity impacts of a low-mass projectile was studied. The same experimental campaign was performed also for the other sandwich structure based on synthetic foam. The residual velocity of the projectile after perforation is shown in Figure 16 for
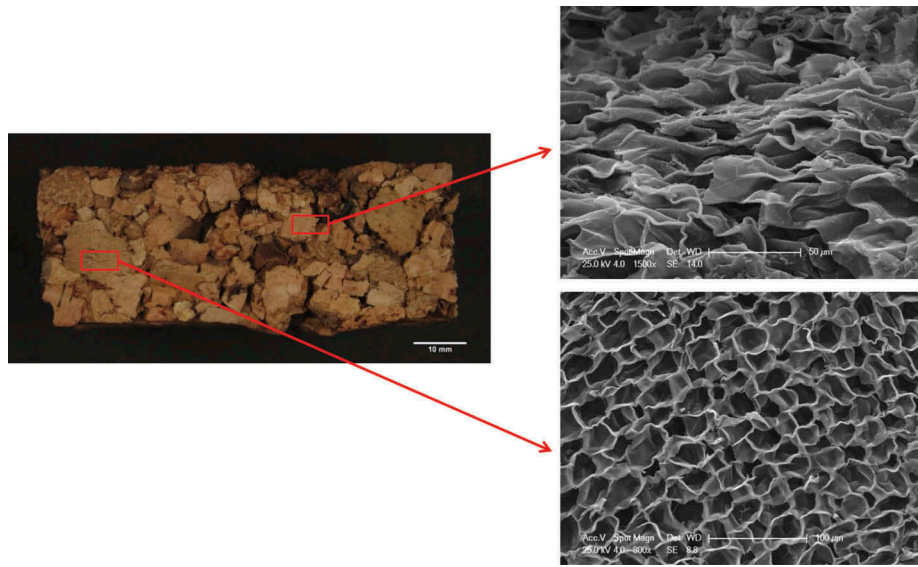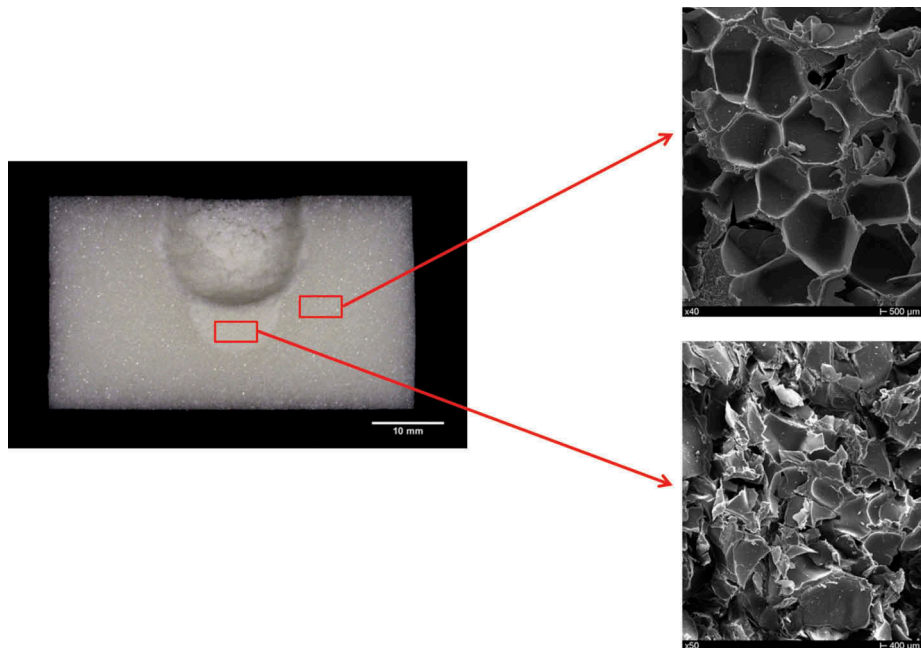
Figure 12. SEM micrographs of bare (a) cork and (b) synthetic foam tested at 75% $E_{\mathrm{p.}}$

both sandwich structures along with the value of the ballistic limit that was not evaluated in a deterministic way but through the well-known Lambert–Jonas model (Buitrago, García-Castillo, and Barbero 2013; Kasano 1999). Good correlation, (Figure 16) was found in the fitting of this model to the experimental data in both sandwiches, with a coefficient of correlation higher than 0.998. Due to the
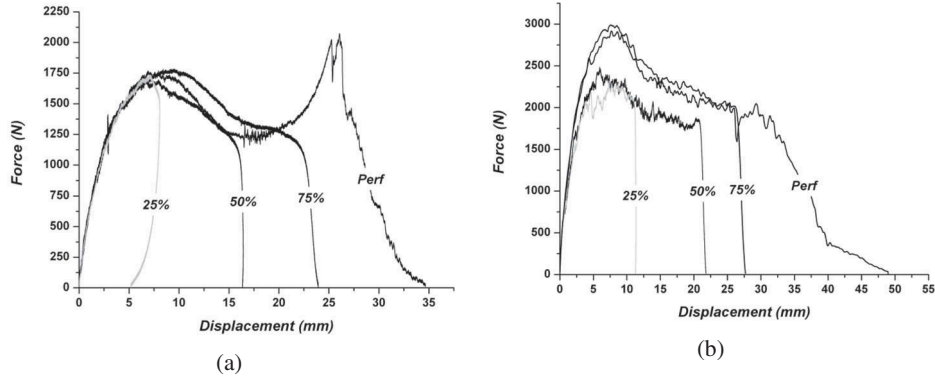
Figure 13. Typical force versus displacement curves of sandwich structures with (a) agglomerated cork and (b) synthetic foam impacted at different energy levels.

different density of both cores, the absorbed energy cannot be compared directly; therefore, the efficiency energy absorption (*EEA*) ratio can be defined as follows (Equation 1):

$$EEA = \frac{\xi}{\rho_A} \qquad (1)$$

where ρ_A is the areal density of the sandwich plate (kg/m^2) while the percentage of the impact energy absorbed (ξ) by each sandwich can be estimated from Equation 2:

$$\xi = \frac{\frac{1}{2} m_p \left(v_i^2 - v_r^2 \right)}{\frac{1}{2} m_p v_i^2} \qquad (2)$$

where m_p is the projectile mass, v_i is the impact velocity, and v_r is the residual velocity. Figure 17 shows EEA ratio as a function of the impact energy for both types of cores. Taking into consideration the differences in areal density, the cork-based sandwich presents a comparable if not slightly better energy absorption capability than the Rohacell-based sandwich. The differences in percentage between the residual velocities of both sandwich structures (residual velocity in Rohacell sandwich–residual velocity in cork sandwich) have been calculated and reported in Figure 18. It is possible to note that when the impact velocity is close to the ballistic limit of the cork sandwich the differences in residual velocities are significant while, with increasing impact velocity, differences decrease asymptotically to 7%.

At high-velocity impact, the whole structural response of the plate is not relevant (Abrate 2005) and the boundary conditions do not affect the ballistic behavior of the plate when the target dimension is large enough compared to the projectile diameter. In this case, a comparison with other core materials is feasible. An important competitor can be represented by polyurethane foams, mainly because of the extensive research on chemicals obtained from renewable resources, such as the production of non-petroleum-derived polyols to be used in polyurethane foams production. In this regard, several processes such as oxypropylation and acid liquefaction of several biomass residues (starch, soybean, alginic acid, palm, sugarcane bagasse, lignin, coffee grounds and even cork) have been proposed over the years (Pawar et al. 2016; Stanzione et al. 2016). Uddin et al. (2009) improved ballistic performance of polyurethane foam by reinforcing it with nanoscale TiO$_2$ particles. The authors reported, for sandwich with nanophased cores and glass fiber/epoxy face sheets, a 20% higher kinetic energy absorption than their neat counterpart with a corresponding increase in ballistic limit around 12% over the neat control samples. The ballistic limit per areal density (m^3/kg-s) was 22.39, which compares quite favorably with the one obtained in the present study for cork-based composites, namely 17.37 m^3/kg-s, especially if differences in face sheets and
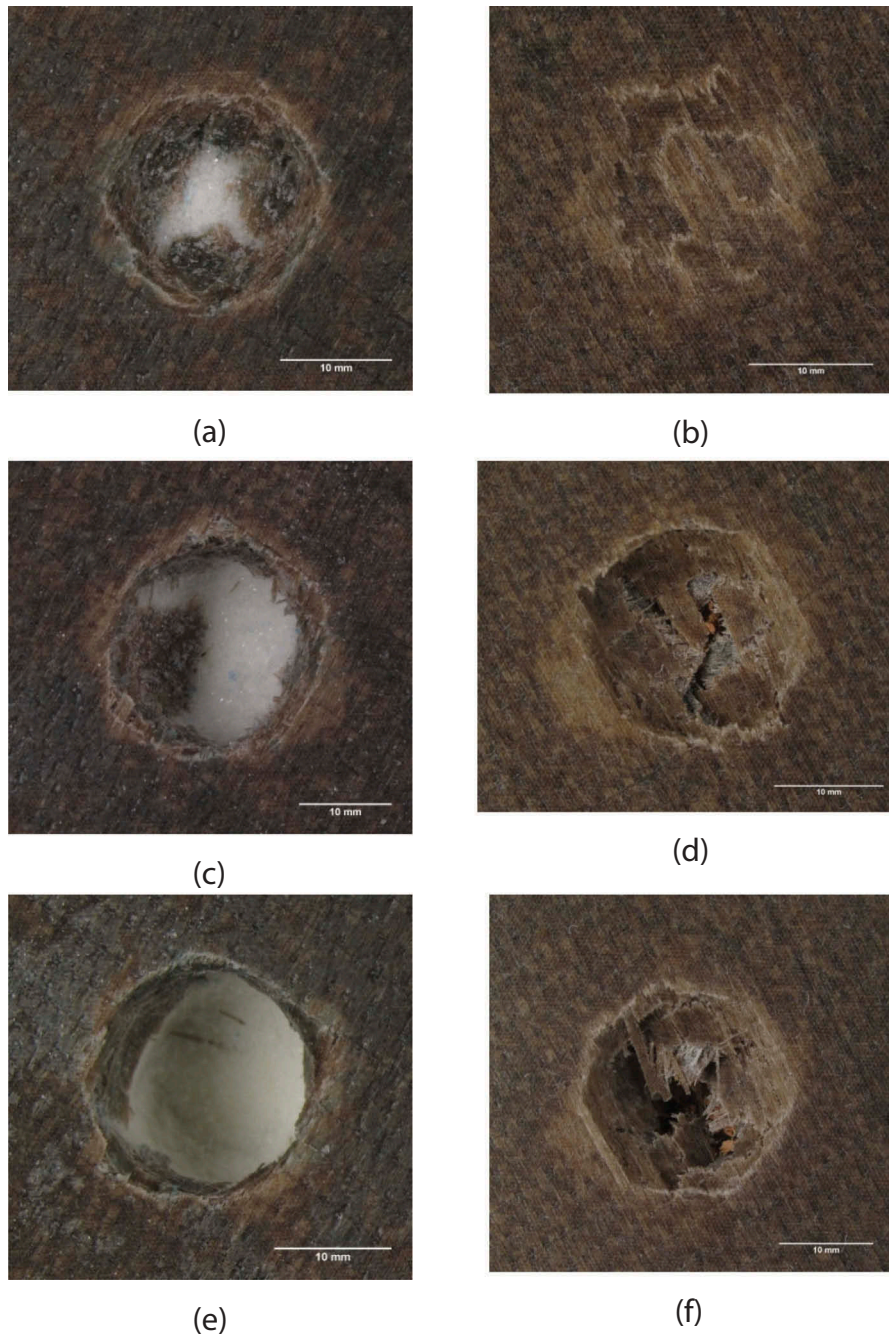
Figure 14. Close-up views of the damage progression in the front surfaces of sandwich structures based on (a, c, e) synthetic foam and (b, d, f) cork impacted from 25% to 75% E_p (from top to bottom).

projectile geometry and mass are taken into consideration. Nasirzadeh and Sabet (2016, 2014) investigated the effect of polyurethane foam density variations in sandwich structure under high-velocity impact loadings. The sandwich consisted of composite face sheets made of glass fibers in unsaturated polyester resin and rigid polyurethane foam core with density of 37, 49, 70, 95, 105, and
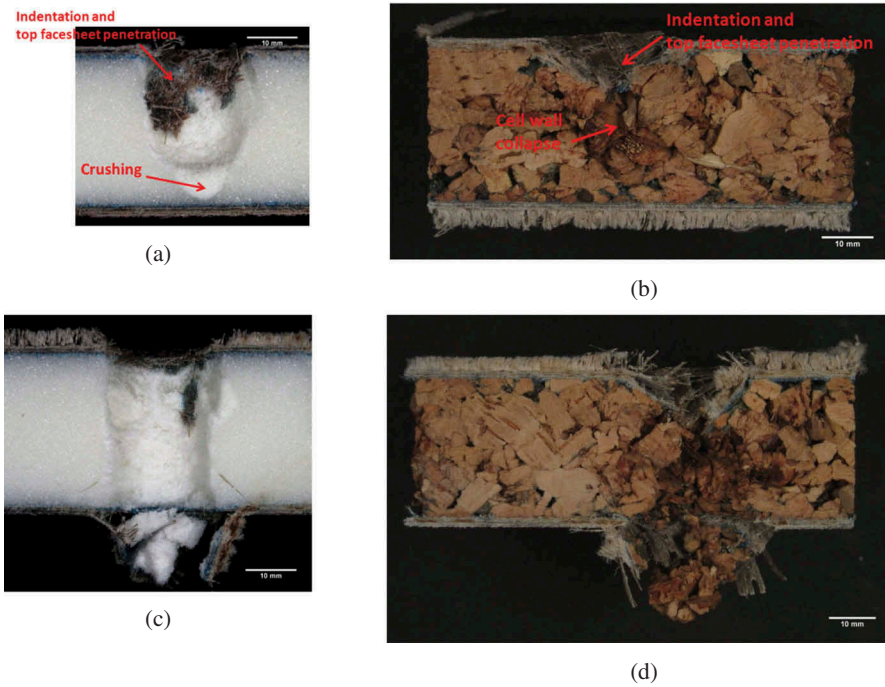
Figure 15. Cross-sectional views of sandwich structures based on (a–c) synthetic foam and (b–d) cork impacted at 75% E_p and at perforation (from top to bottom).
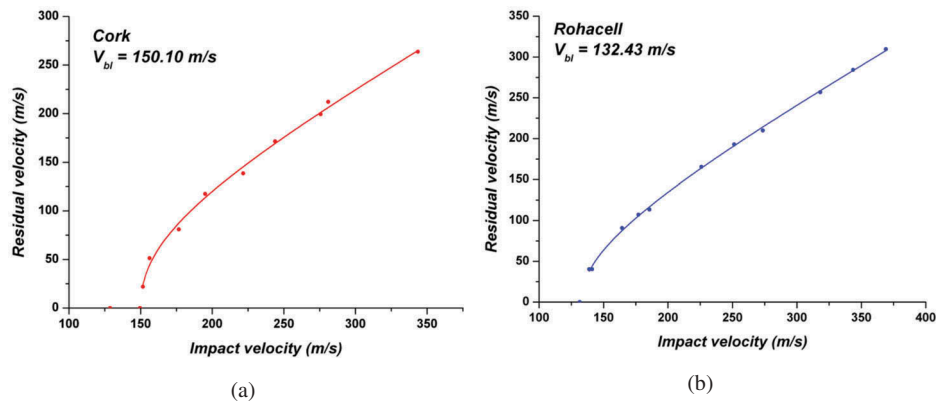

Figure 16. Residual velocity vs. impact velocity of sandwich structures with (a) cork and (b) synthetic foam as core material.

240 kg/m^3. The highest ballistic limit velocity was obtained for specimens with foam core density of 49 kg/m^3, while the lowest ballistic limit velocity was for sandwich panel with foam core density of 240 kg/m^3. This behavior was ascribed to the increased brittle nature of the foam core with the highest density. In all cases, the ballistic limit was fund to lie in the range 100–120 m/s, which is comparable to the one obtained in the present study, even after nanoclay addition in the polyurethane foam core (Nasirzadeh and Sabet 2016).
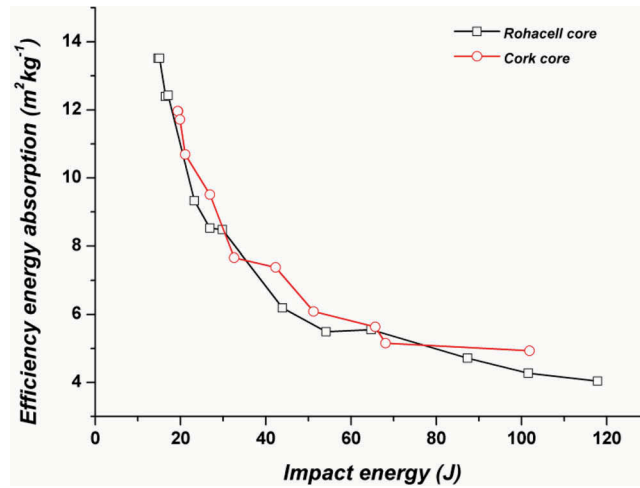
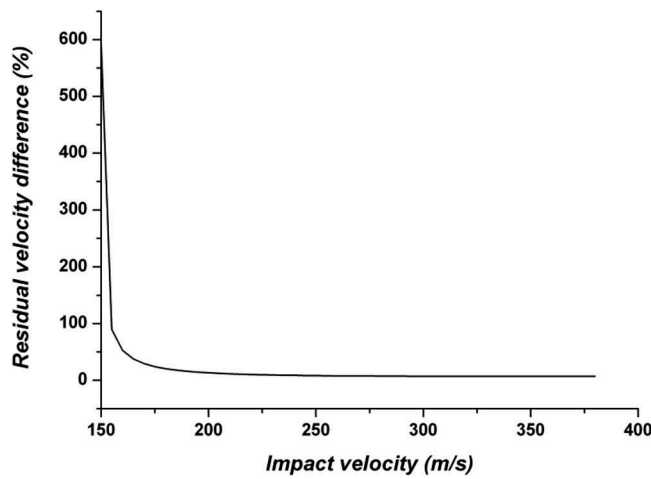**Figure 17.** EEA as a function of impact energy and core type.

Figure 18. Residual velocity difference as a function of impact velocity.

Conclusions

The damage resistance of new sandwich structures with agglomerated cork as core and flax/epoxy laminates as face sheets subjected to low- and high-velocity impacts has been investigated experimentally and compared with a similar sandwich having a synthetic foam as core, namely Rohacell® 110WF. Three samples of each set were tested under impact loading at different percentages of the respective perforation energy, namely 25%, 50%, and 75%. Impact response of the samples was recorded and analyzed, while optical and SEM studies were performed to understand the failure and deformation behavior. The results showed that agglomerated cork can be a renewable alternative to traditional synthetic foam materials because of its inherent and peculiar mechanical behavior. In particular, the collapse of cell walls can be effectively exploited for the absorption of high amount of energy with a limited extension of damage inside the core material. The use of agglomerated cork in a structure made of two thin flax/epoxy laminates resulted also in a normalized ballistic limit

comparable to that offered by synthetic foam materials. The present study suggests also that there is room for improvement, especially in terms of peak loads and perforation energies, which were found to be lower than those offered by high performance and much more expensive synthetic core materials by taking advantage of the flexibility of agglomerated cork in selection from a broad range of densities and grain sizes.

ORCID

S. Sanchez-Saez http://orcid.org/0000-0002-6021-4284

References

Abrate, S. 1997. Localized impact on sandwich structures with laminated facings. *Applied Mechanics Reviews* 50(2):69. doi:10.1115/1.3101689.

Abrate, S. 2005. *Impact on composite structures*. New York, NY: Cambridge University Press.

Akampumuza, O., P. M. Wambua, A. Ahmed, L. Wei, and X. Qin. 2016 February. Review of the applications of biocomposites in the automotive industry. *Polymer Composites* n/a-n/a. doi:10.1002/pc.23847.

Alcântara, I., F. Teixeira-Dias, and M. Paulino. 2013. Cork composites for the absorption of impact energy. *Composite Structures* 95:16–27. doi:10.1016/j.compstruct.2012.07.015.

Barbosa, A. Q., L. F. M. Da Silva, J. Abenojar, M. Figueiredo, and A. Öchsner. 2017. Toughness of a brittle epoxy resin reinforced with micro cork particles: Effect of size, amount and surface treatment. *Composites Part B: Engineering* 114 (April). Elsevier: 299–310. doi:10.1016/J.COMPOSITESB.2016.10.072.

Buitrago, B. L., S. K. García-Castillo, and E. Barbero. 2013. Influence of shear plugging in the energy absorbed by thin carbon-fibre laminates subjected to high-velocity impacts. *Composites Part B: Engineering* 49:86–92. doi:10.1016/j.compositesb.2013.01.005.

Castro, O., J. M. Silva, T. Devezas, A. Silva, and L. Gil. 2010. Cork agglomerates as an ideal core material in lightweight structures. *Materials & Design* 31(1):425–32. doi:10.1016/j.matdes.2009.05.039.

de Moura, M. F. S. F., P. M. L. C. Cavaleiro, F. G. A. Silva, and N. Dourado. 2017. Mixed-mode I+II fracture characterization of a hybrid carbon-epoxy/cork laminate using the single-leg bending test. *Composites Science and Technology* 141 (March). Elsevier: 24–31. doi:10.1016/J.COMPSCITECH.2017.01.001.

de Moura, M. F. S. F., R. Fernandes, F. G. A. Silva, and N. Dourado. 2015. Mode II fracture characterization of a hybrid cork/carbon-epoxy laminate. *Composites Part B: Engineering* 76(July):44–51. doi:10.1016/j.compositesb.2015.02.010.

Faruk, O., A. K. Bledzki, H.-P. Fink, and M. Sain. 2012. Biocomposites reinforced with natural fibers: 2000–2010. *Progress in Polymer Science* 37 (11). Elsevier Ltd: 1552–96. doi:10.1016/j.progpolymsci.2012.04.003.

Fernandes, F. A. O., R. J. S. Pascoal, and R. J. Alves de Sousa. 2014. Modelling impact response of agglomerated cork. *Materials & Design* 58:499–507. doi:10.1016/j.matdes.2014.02.011.

Fowler, P. A., J. Mark Hughes, and R. M. Elias. 2006. Biocomposites: Technology, environmental credentials and market forces. *Journal of the Science of Food and Agriculture* 86 (12). John Wiley & Sons, Ltd.: 1781–89. doi:10.1002/jsfa.2558.

Gameiro, C. P., J. Cirne, and G. Gary. 2007. Experimental study of the quasi-static and dynamic behaviour of cork under compressive loading. *Journal of Materials Science* 42 (12). Kluwer Academic Publishers-Plenum Publishers: 4316–24. doi:10.1007/s10853-006-0675-6.

George, J., I. Verpoest, and J. Ivens. 1999. Mechanical properties of flax fibre reinforced epoxy composites. *Die Angewandte Makromolekulare Chemie* 272(1):41–45. doi:10.1002/(SICI)1522-9505(19991201)272:1<41::AID-APMC41>3.0.CO;2-X.

Ghelli, D., and G. Minak. 2011. Low velocity impact and compression after impact tests on thin carbon/epoxy laminates. *Composites Part B: Engineering* 42(7):2067–79. doi:10.1016/j.compositesb.2011.04.017.

Gibson, L. J., and M. F. Ashby. 1999. *Cellular solids*, 2nd ed. New York, NY: Cambridge University Press.

Goutianos, S., T. Peijs, B. Nystrom, and M. Skrifvars. 2006. Development of flax fibre based textile reinforcements for composite applications. *Applied Composite Materials* 13 (4). Springer Netherlands: 199–215. doi:10.1007/s10443-006-9010-2.

Gurunathan, T., S. Mohanty, and S. K. Nayak. 2015. A review of the recent developments in biocomposites based on natural fibres and their application perspectives. *Composites Part A: Applied Science and Manufacturing* 77 (June):1–25. doi:10.1016/j.compositesa.2015.06.007.

Hachemane, B., R. Zitoune, B. Bezzazi, and C. Bouvet. 2013. Sandwich composites impact and indentation behaviour study. *Composites Part B: Engineering* 51:1–10. doi:10.1016/j.compositesb.2013.02.014.

Jardin, R. T., F. A. O. Fernandes, A. B. Pereira, and R. J. Alves de Sousa. 2015. Static and dynamic mechanical response of different cork agglomerates. *Materials & Design* 68:121–26. doi:10.1016/j.matdes.2014.12.016.

Kasano, H. 1999. Recent advances in high-velocity impact perforation of fiber composite laminates. *JSME International Journal Series A* 42 (2). The Japan Society of Mechanical Engineers: 147–57. doi:10.1299/jsmea.42.147.

Ku, H., H. Wang, N. Pattarachaiyakoop, and M. Trada. 2011. A review on the tensile properties of natural fiber reinforced polymer composites. *Composites Part B: Engineering* 42(4):856–73. doi:10.1016/j.compositesb.2011.01.010.

Lambert, J. P., and G. H. Jonas. 1976. *Towards standardization in terminal ballistics testing: Velocity representation*, Maryland, USA: USA Ballistic Research Laboratories.

Mancuso, A., G. Pitarresi, and D. Tumino. 2015. Mechanical behaviour of a green sandwich made of flax reinforced polymer facings and cork core. *Procedia Engineering* 109:144–53. Elsevier. doi:10.1016/j.proeng.2015.06.225.

Meredith, J., S. R. Coles, R. Powe, E. Collings, S. Cozien-Cazuc, B. Weager, J. Müssig, and K. Kirwan. 2013. On the static and dynamic properties of flax and cordenka epoxy composites. *Composites Science and Technology* 80 (May):31–38. doi:10.1016/j.compscitech.2013.03.003.

Mittal, V., R. Saini, and S. Sinha. 2016. Natural fiber-mediated epoxy composites – A review. *Composites Part B: Engineering* 99:425–35. doi:10.1016/j.compositesb.2016.06.051.

Moreira, R. A. S., F. J. Q. De Melo, and J. F. Dias Rodrigues. 2010. Static and dynamic characterization of composition cork for sandwich beam cores. *Journal of Materials Science* 45 (12). Springer US: 3350–66. doi:10.1007/s10853-010-4356-0.

Nasirzadeh, R., and A. R. Sabet. 2014. Study of foam density variations in composite sandwich panels under high velocity impact loading. *International Journal of Impact Engineering* 63 (January). Pergamon: 129–39. doi:10.1016/J.IJIMPENG.2013.08.009.

Nasirzadeh, R., and A. R. Sabet. 2016. Influence of nanoclay reinforced polyurethane foam toward composite sandwich structure behavior under high velocity impact. *Journal of Cellular Plastics* 52 (3). SAGE PublicationsSage UK: London, England: 253–75. doi:10.1177/0021955X14557104.

Oliveira, V. M., E. Rosa, and H. Pereira. 2014. Variability of the compression properties of cork. *Wood Science and Technology* 48 (5). Springer Berlin Heidelberg: 937–48. doi:10.1007/s00226-014-0651-2.

Paulino, M., and F. Teixeira-Dias. 2011. An energy absorption performance index for cellular materials – Development of a side-impact cork padding. *International Journal of Crashworthiness* 16 (2). Taylor & Francis Group: 135–53. doi:10.1080/13588265.2010.536688.

Pawar, M. S., A. S. Kadam, P. C. Singh, V. V. Kusumkar, and O. S. Yemul. 2016. Rigid polyurethane foams from cottonseed oil using bio-based chain extenders: A renewable approach. *Iranian Polymer Journal* 25 (1). Springer Berlin Heidelberg: 59–68. doi:10.1007/s13726-015-0401-9.

Pereira, H. 2007. *Cork: Biology, production and uses*. The Netherlands: Elsevier.

Petit, S., C. Bouvet, A. Bergerot, and J.-J. Barrau. 2007. Impact and compression after impact experimental study of a composite laminate with a cork thermal shield. *Composites Science and Technology* 67(15):3286–99. doi:10.1016/j.compscitech.2007.03.032.

Phillips, S., J. Baets, L. Lessard, P. Hubert, and I. Verpoest. 2013. Characterization of flax/epoxy prepregs before and after cure. *Journal of Reinforced Plastics and Composites* 32(11):777–85. doi:10.1177/0731684412473359.

Reis, L., and A. Silva. 2009. Mechanical behavior of sandwich structures using natural cork agglomerates as core materials. *Journal of Sandwich Structures and Materials* 11 (6). SAGE Publications: 487–500. doi:10.1177/1099636209104523.

Reis, P. N. B., J. A. M. Ferreira, F. V. Antunes, and J. D. M. Costa. 2007. Flexural behaviour of hybrid laminated composites. *Composites Part A: Applied Science and Manufacturing* 38(6):1612–20. http://www.sciencedirect.com/science/article/pii/S1359835X06003587.

Richardson, M. O. W., and M. J. Wisheart. 1996. Review of low-velocity impact properties of composite materials. *Composites Part A: Applied Science and Manufacturing* 27 (12). Elsevier: 1123–31. doi:10.1016/1359-835X(96)00074-7.

Sanchez-Saez, S., E. Barbero, and J. Cirne. 2011. Experimental study of agglomerated-cork-cored structures subjected to ballistic impacts. *Materials Letters* 65(14):2152–54. doi:10.1016/j.matlet.2011.04.083.

Sanchez-Saez, S., E. Barbero, S. K. Garcia-Castillo, I. Ivañez, and J. Cirne. 2015. Experimental response of agglomerated cork under multi-impact loads. *Materials Letters* 160:327–30. doi:10.1016/j.matlet.2015.08.012.

Sanchez-Saez, S., S. K. García-Castillo, E. Barbero, and J. Cirne. 2015. Dynamic crushing behaviour of agglomerated cork. *Materials & Design* 65:743–48. doi:10.1016/j.matdes.2014.09.054.

Sarasini, F., J. Tirillò, S. D'Altilia, T. Valente, C. Santulli, F. Touchard, L. Chocinski-Arnault, D. Mellier, L. Lampani, and P. Gaudenzi. 2016. Damage tolerance of carbon/flax hybrid composites subjected to low velocity impact. *Composites Part B: Engineering* 91:144–53. doi:10.1016/j.compositesb.2016.01.050.

Sargianis, J., H.-I. Kim, and J. Suhr. 2012. Natural cork agglomerate employed as an environmentally friendly solution for quiet sandwich composites. *Scientific Reports* 2:403. Nature Publishing Group. doi:10.1038/srep00403.

Silva, F. G. A., M. F. S. F. De Moura, and A. G. Magalhães. 2017. Low velocity impact behaviour of a hybrid carbon-epoxy/cork laminate. *Strain* 53(6):e12241. doi:10.1111/str.12241.

Silva, S. P., M. A. Sabino, E. M. Fernandes, V. M. Correlo, L. F. Boesel, and R. L. Reis. 2005. Cork: Properties, capabilities and applications. *International Materials Reviews* 50 (6). Taylor & Francis: 345–65. doi:10.1179/174328005X41168.

Sousa-Martins, J., D. Kakogiannis, F. Coghe, B. Reymen, and F. Teixeira-Dias. 2013. Behaviour of sandwich structures with cork compound cores subjected to blast waves. *Engineering Structures* 46:140–46. doi:10.1016/j.engstruct.2012.07.030.

Stanzione, M., V. Russo, A. Sorrentino, R. Tesser, M. Lavorgna, M. Oliviero, M. Di Serio, S. Iannace, and L. Verdolotti. 2016. Bio-based polyurethane foams from renewable resources. In *AIP Conference Proceedings*, 1736: 020130. AIP Publishing LLC. doi:10.1063/1.4949705.

Tita, V., J. de Carvalho, and D. Vandepitte. 2008. Failure analysis of low velocity impact on thin composite laminates: experimental and numerical approaches. *Composite Structures* 83(4):413–28. doi:10.1016/j.compstruct.2007.06.003.

Triantou, K., B. Perez, A. Marinou, S. Florez, K. Mergia, G. Vekinis, J. Barcena, W. Rotärmel, C. Zuber, and À. de Montbrun. 2017. Performance of cork and ceramic matrix composite joints for re-entry thermal protection structures. *Composites Part B: Engineering* 108 (January). Elsevier: 270–78. doi:10.1016/J.COMPOSITESB.2016.09.104.

Uddin, M. F., H. Mahfuz, S. Zainuddin, and S. Jeelani. 2009. Improving ballistic performance of polyurethane foam by nanoparticle reinforcement. *Journal of Nanotechnology* (January):1–8. Hindawi. doi:10.1155/2009/794740.

Walsh, J., H.-I. Kim, and J. Suhr. 2017. Low velocity impact resistance and energy absorption of environmentally friendly expanded cork core-carbon fiber sandwich composites. *Composites Part A: Applied Science and Manufacturing* 101 (October). Elsevier: 290–96. doi:10.1016/J.COMPOSITESA.2017.05.026.

Wang, J., A. M. Waas, and H. Wang. 2013. Experimental and numerical study on the low-velocity impact behavior of foam-core sandwich panels. *Composite Structures* 96:298–311. http://www.sciencedirect.com/science/article/pii/S026382231200428X.

Zenkert, D., A. Shipsha, P. Bull, and B. Hayman. 2005. Damage tolerance assessment of composite sandwich panels with localised damage. *Composites Science and Technology* 65(15):2597–611. doi:10.1016/j.compscitech.2005.05.026.

Zhou, J., Z. W. Guan, W. J. Cantwell, M. Meo, A. J. Morris, R. Vignjevic, G. Marengo, et al. 2012. The perforation resistance of sandwich structures subjected to low velocity projectile impact loading. *The Aeronautical Journal* 116 (1186):1247–62. Cambridge University Press. doi:10.1017/S0001924000007624.

Zhuang, J., S. H. Ghaffar, M. Fan, and J. Corker. 2017. Restructure of expanded cork with fumed silica as novel core materials for vacuum insulation panels. *Composites Part B: Engineering* 127 (October). Elsevier: 215–21. doi:10.1016/J.COMPOSITESB.2017.06.019.